

## Article

# Research Progress on Polyaniline-Ionic liquids for Long Cycle-Stable Supercapacitors with High Capacitance

Fatima AL-ZOHBI

Laboratoire Matériaux, Catalyse, Environnement et Méthodes Analytiques (MCEMA) Campus Universitaire de Hadath, Liban;

\* Correspondence: [alzohbi-fatima@hotmail.com](mailto:alzohbi-fatima@hotmail.com); Tel.: +961 (0)6 83 55 24 (F. A)

Received: Feb 14, 2022; Accepted: Mar 14, 2022; Published: Mar 30, 2022

**Abstract:** Ionic liquids have been used either as polymerization medium or as electrolytes for polyaniline (PANI) electrodes to produce long cycle-stable supercapacitors with high capacitance. As a polymerization medium, ionic liquids play the role of a soft template agent and induce the formation of nanostructured PANI morphology. Nanorod, nanowire, or spherical PANI morphology has been obtained in ionic liquids instead of agglomerated particles resulted in the conventional media. The well-defined one-dimensional PANI morphology ensures a short charge transfer distance in the PANI materials and low contact resistance between PANI and electrolyte interfaces. The efficiency of ionic liquids as a soft template agent is related to their structure as well as to their proportion in the reaction medium. As electrolytes, “neat” ionic liquids provide low but stable specific capacitance of PANI over more than hundreds of cycles. Binary mixtures of ionic liquids and solvents (e.g. acetonitrile, water) have increased both the specific capacitance and the capacitance retention of PANI compared with the performances resulting in the conventional aqueous acid electrolytes. Using ionic liquids to carry out both the synthesis and the electrochemical characterization of PANI is an effective approach to improve PANI cycle life. The key parameter is to choose the convenient ionic liquids. This review covers the most significant studies conducted on PANI/ionic liquids for supercapacitor applications.

**Keywords:** Polyaniline (PANI), Ionic liquids, Supercapacitors, Cycle life

## 1. Introduction

Supercapacitors, also known as ultracapacitors, are electrochemical energy storage devices that have become an essential daily need in our life [1–3]. They are used either on their own or in conjunction with batteries (e.g. superbattery) [3–5]. Supercapacitors are made up of a positive and a negative side, called electrodes, separated from each other by an ion-permeable separator material and an electrolyte. Their charge storage mechanisms are related to the electrode materials, which are divided into three categories as follows [6–12].

- **Electric double-layer capacitors (EDLCs)** are typically based on carbon derivatives and store charge through electrostatic adsorption of ions at the electrode/electrolyte interface.
- **Pseudocapacitors** are based not only on metal oxides/hydroxides but also on conducting polymer and storing charge mainly electrochemically.
- **Hybrid capacitors** are based on asymmetric electrodes of different types.

Supercapacitors almost follow the same design, and each type has its benefits and drawbacks [10–12]. Electric double-layer capacitor (EDLC) is the most popular in the supercapacitor market since they provide instantaneous high power density with good cycle life and fast charge/discharge rate. In contrast, its low energy density and its self-discharge are barriers to a wide range of use [13]. Concerning hybrid capacitors, they have not had commercial success as they are non-reliable and cannot be fully discharged [14]. Pseudocapacitors are a potential candidate to be an alternative to EDLCs since they literally keep the features of EDLCs and, additionally, hold high energy density.

One of the most investigated electrode materials for pseudocapacitors is polyaniline (PANI), which is a conducting polymer with organic semiconductors' properties and a large surface area [7,12,15–24]. PANI electrodes are characterized by a high theoretical mass specific capacitance (*ca.* 750 F/g), good thermal stability, high electronic conductivity (at its doped state), and low cost owing to simple synthesis [7,12,15–24]. Another characteristic of PANI is that it stores electrochemical energy through a fast reversible redox process [25–28]. On the other side, PANI electrodes exhibit limited cycle life and stability in conventional aqueous acid electrolytes (H<sub>2</sub>SO<sub>4</sub>, HCl, and others) because of the intercalation/deintercalation of electrolytes ions into PANI chains [29–

31]. To improve the cycle life of PANI electrodes, conventional aqueous electrolytes have been replaced by ionic liquids in recent studies [16, 32–46].

Ionic liquids are salts with a melting point of less than 100 °C. They are investigated as electrolytes as well as polymerization media for PANI. As electrolytes, ionic liquids have attracted attention owing to their wider potential window as compared with conventional solvents [47]. As polymerization media, ionic liquids are considered green solvents owing to thermal and chemical stability, negligible volatility, non-corrosively, low cost, low flammability, and nontoxicity features. Two main subclasses of ionic liquids are mostly used in the studies on the combination of PANI and ionic liquids such as aprotic ionic liquids (AILs) and protic ionic liquids (PILs) [48]. These subclasses differ from each other by the availability of labile proton (the presence and the absence of labile hydrogen for PILs and AILs, respectively) and by their transport properties (neat AILs are generally more conductive and less viscous than neat PILs) [43,49,50].

This article comprises four sections. In the first section, we show the synthesis conditions to obtain PANI films by electrodeposition in ionic liquids. Secondly, we discuss the effect of ionic liquids as polymerization medium on PANI morphology and its related properties in the second section. In the third section, we present how ionic liquid-based electrolytes affect the electrochemical performances as well as the charge storage mechanism of PANI electrodes. Finally, all ionic liquids used for synthesis or electrochemical evaluation of PANI material are listed.

## 2. Ionic liquids for electrochemical synthesis of PANI: PILs vs AILs

Electropolymerization of aniline in solvent-free ionic liquids is considered a solution to prevent side reactions due to electrolyte-solvent electrolysis during the polymerization, as ionic liquids exhibit more electrochemical stability than molecular solvents [45,51–53]. According to Refs. [52,53], PILs with high proton activity are appropriate for the electropolymerization of aniline. However, AILs require an exogenous proton source (extra acid or pre-protonated aniline) to achieve this electropolymerization.

Wei *et al.* showed that the electropolymerization of aniline was possible in 1-butyl-3-methylimidazolium hexafluorophosphate (BMIPF<sub>6</sub>) mixed with 1 mol/l trifluoroacetic acid, which was a source of necessary protons for aniline electropolymerization [51]. In other work, Snook *et al.* demonstrated that it was impossible to prepare PANI film from aniline in neat 1-butyl-1-methylpyrrolidinium bis (trifluoro-methane-sulfonyl) imide (C<sub>4</sub>mpyrTFSI), which do not have enough excess protons [45]. To obtain the polymerization reaction, pre-protonated aniline (*i.e.* anilinium nitrate) was used as an alternative to aniline. Therefore, the polymerization takes place without the need for another proton source [45].

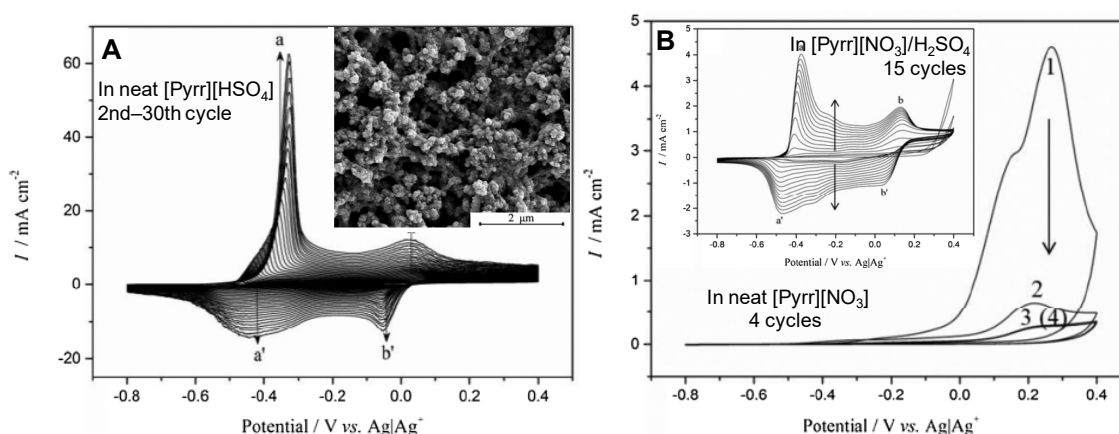
A comparative study on the electropolymerization of anilinium nitrate was carried out with PIL (*i.e.* ethyl ammonium nitrate (EAN) with pH *ca.* 5) and AIL (*i.e.* C<sub>4</sub>mpyrTFSI of low proton activity) to study the possible suitability of each media [45]. The electrodeposition was conducted by cyclic voltammetry in a three-electrode system with a platinum disk (100 μm diameter) as a working electrode. The study result showed that the deposition of PANI was possible in both ionic liquids. However, the resulting PANI film thickness was different. A thin film was obtained in C<sub>4</sub>mpyrTFSI but EAN led to thick and porous films [45]. This difference is due to the limited solubility of anilinium in C<sub>4</sub>mpyrTFSI (much less than 300 mM) while the concentration solution of anilinium nitrate in EAN was 380 mM. The electrochemical performances of PANI film obtained in EAN were then studied by cyclic voltammetry in neat EAN. This film exhibited a relatively high specific capacitance of over 0.6 F/cm<sup>2</sup> at 20 mV/s with up to 4 C/cm<sup>2</sup> deposited charges [45].

In terms of the quality of PANI films obtained using EAN, Shen *et al.* compared the electropolymerization of aniline in two PILs with different anions namely pyrrolidinium hydrogen sulfate ((Pyr)HSO<sub>4</sub>) and pyrrolidinium nitrate ((Pyr)NO<sub>3</sub>) [53]. **Fig. 1 A** shows the CV cycles during the anodic deposition of PANI. The CV experiment was conducted in neat (Pyr)HSO<sub>4</sub>, and the voltage scan (forward and backward scans) was repeated for 30 scans. During the forward scan, aniline started to oxidize and thus polymerize at a relative potential around -0.5 V. The resulting polymer settled down on the electrode by changing its electrochemical response. During the backward scan, the potential reduction peaks (a' and b'), related to the p-dedoping of the polymer, were observed since the first CV cycle and its current increased during the following CV cycles. The oxidation peaks (a and b) are related to the doping process of PANI. Furthermore, the p-doping and dedoping processes were highly reversible as evidenced by the two pairs of redox (a, a' and b, b') peaks. The oxidation peak corresponds to the leucoemeraldine and emeraldine salts, and the reduction peaks are attributed to by the leucoemeraldine and emeraldine base. The obtained PANI exhibited a nanoporous morphology as evidenced by the SEM image shown in the inset of **Fig. 1A**. However, in neat (Pyr)(NO<sub>3</sub>), the CV of aniline did not display the redox peaks of PANI (**Fig. 1B**), indicating the inability to electropolymerize aniline in neat (Pyr)NO<sub>3</sub>. Thus, to obtain the electropolymerization in (Pyr)NO<sub>3</sub>, sulfuric acid was added as an exogenous proton source to the medium. The resulted CV curves of aniline displayed two pairs of redox peaks of PANI as presented in **Fig. 1B**. The electrodeposition of PANI in (Pyr)NO<sub>3</sub> required the presence of H<sub>2</sub>SO<sub>4</sub> due to the low proton activity of neat (Pyr)NO<sub>3</sub>. As a result, the electropolymerization of aniline was possible in neat (Pyr)(HSO<sub>4</sub>) (~ pH 1.9) but this is not the case in neat (Pyr)(NO<sub>3</sub>) (~ pH 6.9), revealing that good proton

activity (*i.e.* high concentration of the proton in the solution) of ionic liquid media is a requested for efficient electropolymerization of aniline. The specific capacitance of the PANI electrode prepared in (Pyrr)(H<sub>2</sub>SO<sub>4</sub>) is estimated to be *ca.* 0.6 F/cm<sup>2</sup> at 20 mV/s with 3.6 C/cm<sup>2</sup> deposited charges (close to that presented by Snook *et al.* [45] under similar conditions).

Patil *et al.* [52] reported that N-methyl-2-pyrrolidonium hydrogensulfate (NMP)(H<sub>2</sub>SO<sub>4</sub>), which has protonated anion, was also an appropriate medium for PANI electrodeposition. In this study, the electropolymerization of aniline was carried out by using a three-electrode system in a 0.1 mol/l (NMP)H<sub>2</sub>SO<sub>4</sub> aqueous medium. It was possible to control the thickness of PANI film from 0.98 to 7.02 μm by varying the deposition cycles from the 1<sup>st</sup> cycle to the 5<sup>th</sup> cycle. The specific capacitance of each film was calculated from CV curves recorded at a 5 mV/s scan rate within a potential window of -0.2 to 0.8 V versus a saturated calomel electrode (SCE) in 0.1 M (NMP)H<sub>2</sub>SO<sub>4</sub> ionic liquid. The specific capacitance increased (from 338 to 581 F/g) along with the increment of the film thickness (from 0.98 to 6.58 μm) then it decreased to 560 F/g for PANI film thickness of 7.02 μm due to the high inherent resistance of PANI.

Recently, deep eutectic solvents (*i.e.* a type of ionic liquid), which are defined by having a melting point that is lower than their components, have been investigated as electropolymerization medium of aniline [54,55]. Ismail *et al.* reported the electrodeposition of PANI in propeline 200 (prepared by combining choline chloride in a 1:2 molar ratio with 1,2- propylene glycol) by cyclic voltammetry with a scan rate of 100 mV/s at 25 °C in the three-electrode system [54]. Pure propeline 200 electrolyte (~pH 7) is not an appropriate medium for the growth of PANI film as this electrolyte does not have protons that participates in the oxidation reaction of aniline. The addition of 1 M H<sub>2</sub>SO<sub>4</sub> to propeline 200 was not effective to induce the polymerization of aniline. For electropolymerization, 10 % volume H<sub>2</sub>O was added to 1 M H<sub>2</sub>SO<sub>4</sub>/propeline 200 as the species diffuse faster in the propeline 200-water solution [54]. Thus, the electropolymerization of aniline requires a highly protonated medium. Hence, PILs with high proton activity are convenient media to achieve the electrodeposition of PANI without the need for an exogenous proton source.



**Fig. 1.** CV curves of aniline (0.3 M) at platinum disk electrode with the scan rate of 20 mV/s (a) in neat (Pyrr)(H<sub>2</sub>SO<sub>4</sub>) (insert image shows the SEM image of the obtained PANI film) and (b) in neat (Pyrr)(NO<sub>3</sub>) (insert figure shows CV curves of aniline in H<sub>2</sub>SO<sub>4</sub> spiked (Pyrr)(NO<sub>3</sub>)) (data are reproduced from Ref. [53], Copyright 2018, Elsevier B.V. )

### 3. Ionic liquids for chemical oxidative polymerization of PANI

PANI has typically been prepared in situ oxidative polymerization of aniline monomer in the conventional aqueous acid media by adding the oxidant agent dropwise. The PANI generally experiences an agglomerated granular particles or inhomogeneous fibrillar morphology, depending on the synthesis conditions such as dopant/aniline molar ratio [56], pH of polymerization media [57–60], polymerization temperature and time [61], stirring conditions [62,63], dopant size and type [16,23, 64–67], and oxidant type [68–70]. As the morphology of PANI largely affects its electrochemical performances [31,33,52,61,71], the conventional acidic media have been replaced by ionic liquids to obtain nanostructured porous materials with a large surface area. Several studies have been carried out using AILs with different aniline to ionic liquid mole ratios [34,35]. Other studies have discussed the effect of AILs structures (*i.e.* alkyl chain length, anion groups, or head group structures) on PANI morphology and related properties [16,35,72,73]. The use of PILs for the synthesis of PANI has been also researched [46,74]. In this section, we present how the composition of ionic liquids (*i.e.* aniline/AIL mole ratio, alkyl chain length of AILs, and the structure of the anions and the cations of AILs), used as polymerization medium, can affect the morphology and the related properties of PANI.

#### 3.1 Aniline/AIL mole ratio

The effect of the molar ratio of aniline to 1-butyl-3-methylimidazolium chloride [bmim]Cl on PANI properties was evaluated through an investigation of PANI prepared via chemical oxidation of aniline in aqueous HCl containing (bmim)Cl [34]. All the experimental conditions were fixed except the molar ratio of aniline to (bmim)Cl [34]. **Table 1** shows a detailed description of the morphology of the obtained PANI as a function of the mole ratio of aniline/(bmim)Cl. The dependence of PANI morphology on aniline/[bmim]Cl mole ratio is notable. When (bmim)Cl was added to a reaction medium, PANI exhibited nanowire morphology instead of agglomerated granular morphology of conventional PANI (aniline/(bmim)Cl mole ratio of 1/0). Nanowire structure was the dominant morphology when the polymer was prepared at the aniline/(bmim)Cl mole ratio equal to 1:1. Then nanowire morphology was replaced by lamellar structure when the ratio of [bmim]Cl was higher than that of aniline (aniline/(bmim)Cl mole ratio equal to 1/2 or 1/4). Despite the dependence of the morphology of PANI on the aniline/(bmim)Cl mole ratio, its structure (determined by Fourier-transform infrared spectroscopy) and molecular-weight characteristics were not affected by the aniline/(bmim)Cl mole ratio. The relationship between PANI morphology and aniline/AIL mole ratio was later confirmed by Pahovnik *et al.*[35] and Zhang *et al.* [75].

**Table 1.** Morphology description of PANI prepared in the presence of (bmim)Cl with different aniline/(bmim)Cl mole ratio (data are adapted from Ref. [34]. Copyright 2010, Elsevier B.V.)

Aniline/(bmim)Cl mole ratio	description of the PANI morphology
1/0	Strongly <i>agglomerated granular</i> morphology
4/1	<i>Granular</i> morphology was dominant ; some <i>nanowires</i> were present
2/1	Increment in the fraction of <i>nanowire</i> morphology
1/1	Only <i>nanowire</i> structure (diameter of 80 – 100 nm)
1/2	<i>Nanowire</i> structure was dominant; <i>Lamellar</i> structure was present
1/4	Leaf-like <i>lamellas</i> was dominant (they were organized into complex three dimensional fan-shaped structures)

### 3.2 AILs chemical structure

The effect of the chemical structure of AILs, including alkyl chain length or the structure of the head groups or the structure of the anion, on PANI morphology, and related properties are described in this section.

#### 3.2.1 AILs Alkyl chain length

1-alkyl-3-carboxymethylimidazolium chloride (RCMIm)Cl (an AIL containing carboxyl group) with different alkyl chain length were used as a polymerization medium for PANI to study the impact of the alkyl chain length on the PANI properties [72]. 1-alkyl-3-methylimidazolium chloride (RMeIm)(Cl) (an AIL without carboxyl group) were also investigated [35].

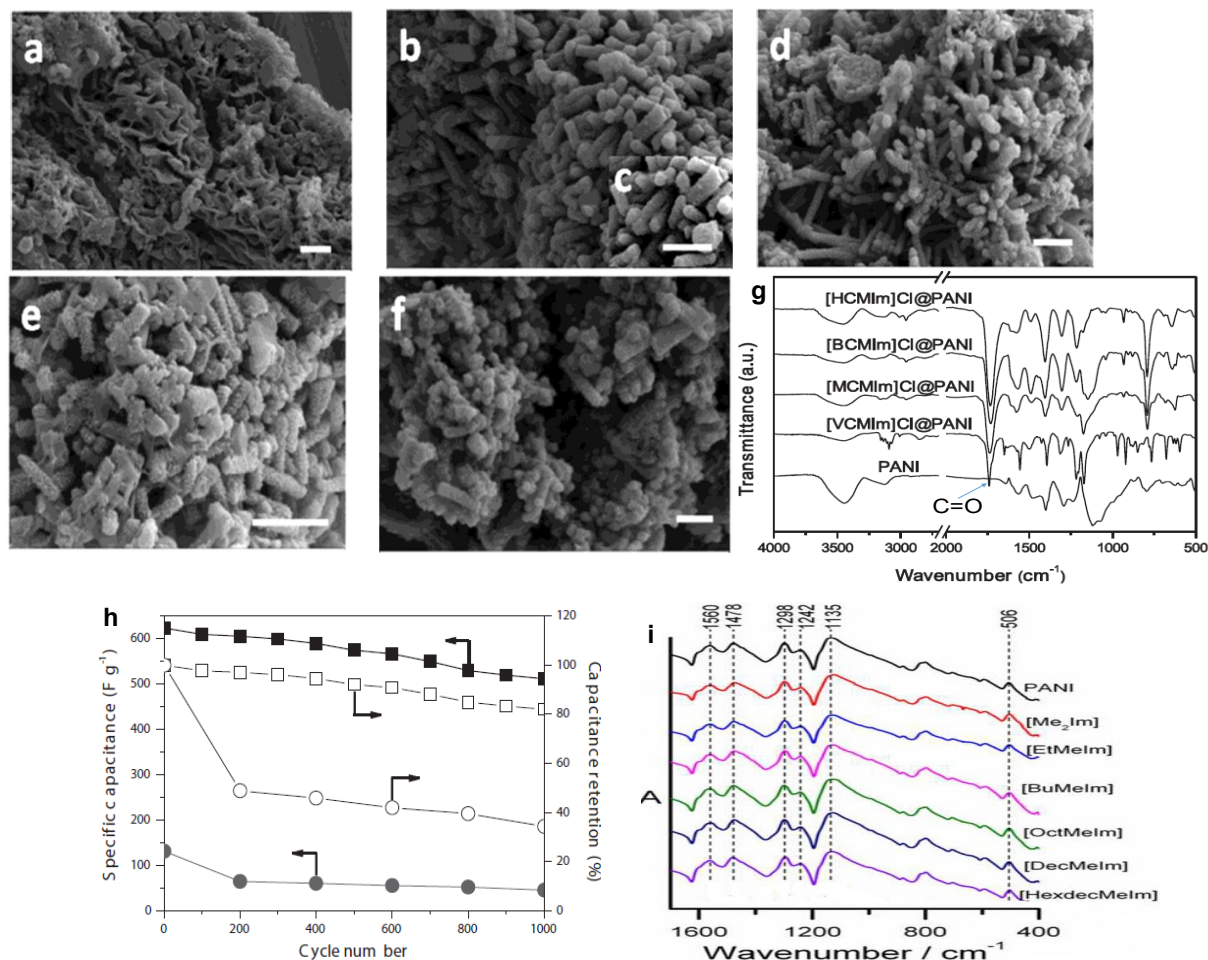
When (RCMIm)Cl (where R was methyl M, vinyl V, allyl A, butyl B1, or hexyl H groups) was added into polymerization medium, the morphology and the electrochemical performances of the obtained PANI were effectively affected by the R group [72]. **Fig. 2** shows the SEM images of PANI obtained in (RCMIm)Cl as well as that of the conventional PANI. Firstly, the significant change in PANI morphology when (RCMIm)Cl was added to the reaction medium. It was petal-like morphology for the conventional PANI (**Fig. 2a**) but maize-like nanorods for (RCMIm)Cl@PANI (**Fig. 2b-f**). The nanorods number decreased along with the increment of alkyl chain length in AILs. The well-organized maize-like structure was obtained in (VCMIm)Cl owing to the interaction between PANI and (VCMIm)Cl (**Fig. 2b**). In addition to the effect of (RCMIm)Cl on the nanostructuring of PANI, (RCMIm)Cl doped PANI was confirmed by FT-IR spectroscopy. **Fig. 2g** compares the FT-IR spectra of (RCMIm)Cl@PANI with that of the conventional PANI. The FT-IR spectra reveal that the spectra of (RCMIm)Cl@PANI displayed the characteristic vibration bands assigned to the ionic liquid in addition to those attributed to by PANI and that (RCMIm)Cl@PANI was doped with the ionic liquids.

The effect of (RCMIm)Cl on the electrochemical performances of PANI was also studied. The electrochemical measurements were carried out using a three-electrode system in H<sub>2</sub>SO<sub>4</sub> 0.5 mol/l. A glassy carbon electrode with a diameter of 3 mm and loaded with 0.10 mg of the thin film of active material (containing one part (by mass) of PANI and 11 parts of 0.5 wt% Nafion). The specific capacitance values, calculated from the galvanostatic charge/discharge at 1 A/g, were as follows: (VCMIm)Cl@PANI (624 F/g) > (ACMIm)Cl@PANI (337 F/g) ≈ (MCMIm)Cl@PANI (331 F/g) > (BCMIm)Cl@PANI (262 F/g) > (HCMIm)Cl@PANI (216 F/g) > conventional PANI (166 F/g). Remarkably, the specific capacitance of (RCMIm)Cl@PANI experienced higher specific capacitance (whatever the alkyl chain length) than the conventional PANI. This enhancement occurs as the imidazole and carboxyl groups in AILs improve the electrode wettability to facilitate the surface reactions of electrode materials. It is also noticeable that



the specific capacitance decreased along with the increment of alkyl chain length of (RCMIm)Cl and the highest value was obtained for (VCMIm)Cl@PANI compared to the other obtained PANI owing to its well-organized morphology.

The capacitance retention of (VCMIm)Cl@PANI electrode material, as well as that of the pristine PANI, are presented in **Fig. 2h**. Only a little decrease in the specific capacitance of (VCMIm)Cl@PANI electrode material was produced before 400 cycles (94.6% of the initial value remained) compared with almost half loss in the capacitance of pristine PANI.



**Fig. 2.** SEM images of PANI nanocomposites with different dopants. (a) HCl, (b) (VCMIm)Cl, (c) magnification of b, (d) (MCMIm)Cl, (e) (BCMIm)Cl, (f) (HCMIm)Cl, All the scale bars are 1  $\mu\text{m}$ , (g) FT-IR spectra of PANI electrodes prepared in (RCMIm)Cl and (h) Variations of the specific capacitance and capacitance retention of PANI electrodes as a function of cycle number based on charge/discharge curves at the current density of 1.0 A/g. (square: (VCMIm)Cl@PANI; circle: pristine PANI) (SEM images, (g) and (h) are from Ref. [72]. Copyright 2019 song et al., published by De Gruyter; (i) is from Ref. [35]. Copyright 2013, Elsevier Ltd)

On the other hand, when (RMeImi)Cl (where R was methyl, ethyl, butyl, octyl, decyl, or hexadecyl) was used as polymerization medium, the morphology of obtained PANI was nanowire [35]. Additionally, the organization of nanowire was strongly related to the alkyl chain length which is attributed to the solubility rate of (RMeImi)Cl after the addition of ammonium peroxydisulfate (oxidant agent) in the synthesis medium. [35]. Thus, the formation of well-defined one-dimensional PANI nanostructured decreased when (RMeImi)Cl with longer alkyl chains in a high concentration was used due to its poor solubility. Opposite to (RCMIm)Cl, (RMeImi)Cl did not dope PANI as shown in FT-IR spectra (**Fig. 2i**). Indeed, the characteristic vibration bands of AILs were not detected, indicating that (RMeImi)Cl was easily washed out of PANI during its purification [35]. Additionally, the FT-IR spectra of PANI prepared in (RMeImi)Cl were superposable with that of the conventional PANI, revealing that the structure and oxidation state of PANI are not affected by (RMeImi)Cl. The alkyl chain length of (RMeImi)Cl did not affect the conductivity of PANI (*i.e.* the conductivity was of the order of 0.2 S/cm regardless of the chain length of AILs) and the number- and mass-average molar masses of PANI [35].

The ionic liquids ((RCMIm)Cl and (RMeImi)Cl) play the role of a soft template agent to organize the morphology of PANI. However, (RMeImi)Cl has a solubility issue with a long alkyl chain while this is not the case for (RCMImi)Cl, revealing that the

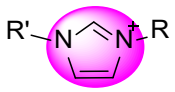

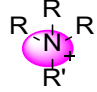
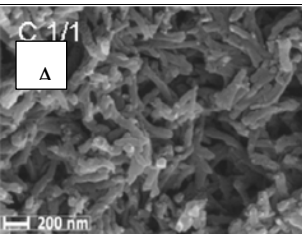
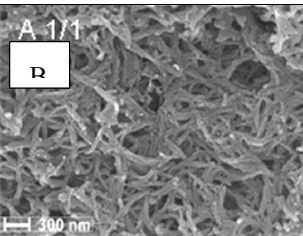
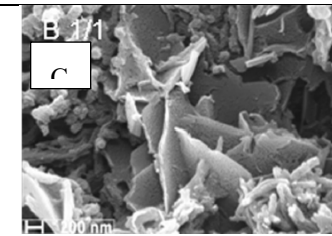
carboxyl group of AIL controls the solubility of AIL in the polymerization medium along with the alkyl chain length and their interaction with PANI chain. In addition, (RCMIm)(Cl) dopes PANI which is not the case of (RMeIm)Cl.

### 3.2.2 AILs cations

The effect of cations of AILs on the morphology, spectroscopic characteristics, and conductivity of PANI were investigated by comparing PANI prepared in an acidic aqueous medium containing pyridinium, imidazolium, or quaternary ammonium-based AIL, namely 1-butyl-3-methylpyridinium chloride ((BuMePyr)Cl), 1-butyl-3-methylimidazolium chloride (BuMeIm)Cl or methyltributylammonium chloride ((Bu<sub>3</sub>MeN)Cl) [35, 73]. **Table 2** shows the structure of cations of (BuMeIm)Cl, (BuMePyr)Cl, or (Bu<sub>3</sub>MeN)Cl and the morphology of the obtained PANI powder. (BuMeIm)Cl and (BuMePyr)Cl induced the formation of nanowire particles of PANI with respect to the uniformity of size and shape instead of agglomerated granular morphology of conventional PANI. This similarity in PANI morphology obtained from both AILs was contributed to by the similar structure of imidazolium and pyridinium cations, which interacts with PANI via  $\pi$ - $\pi$  interactions. However, (Bu<sub>3</sub>MeN)Cl induced the formation of lamellar particles of PANI with a significant amount of irregularly shaped nanoparticles [35]. Quaternary ammonium cation of (Bu<sub>3</sub>MeN)Cl has a charge localized at its nitrogen atom, and its interactions with aniline/anilinium cations are probably different from that of imidazolium or pyridinium. As a result, this leads to differently ordered nanostructures in solution, and consequently, different morphology of formed PANI [35]. Although these AILs acted as a soft template agent in the polymerization medium of PANI, they did not affect either the oxidation states of the formed PANI (as determined by Fourier-transform infrared or UV-visible spectroscopies) nor the conductivity (it was almost 0.2 S/cm) [35, 73].

On the other hand, the replacement of (BuMePyr)Cl or (BuMeIm)Cl by inorganic chlorides (NaCl, CaCl<sub>2</sub>) gave PANI with agglomerated morphology similar to that of conventional PANI, confirming the role of the AILs as a soft template agent [73]. However, the addition of AlCl<sub>3</sub> to the conventional medium promotes the formation of agglomerated elongated particles with a spotted surface [73]. AlCl<sub>3</sub> on PANI morphology, as compared to the conventional PANI, influences the possible electrostatic interaction between (AlCl<sub>4</sub>)<sup>-</sup> (anions formed in situ reaction of AlCl<sub>3</sub> with HCl) and PANI. Furthermore, the additives (NaCl, CaCl<sub>2</sub>, or AlCl<sub>3</sub>) did not affect the oxidation state or the conductivity of PANI [73].

**Table 2** : Structure of AIL cations used for polymerization of PANI (R, butyl group and R', methyl group) and SEM images of PANI samples prepared using aniline/AIL mole ratio equal to 1/1 with: (A) (BuMeIm)Cl, (B) (BuMePyr)Cl and (C) (Bu<sub>3</sub>MeN)Cl (from reference [35])

Investigated AIL	(BuMeIm)Cl	(BuMePyr)Cl	(Bu <sub>3</sub> MeN)Cl
AIL cations			
SEM images of PANI			

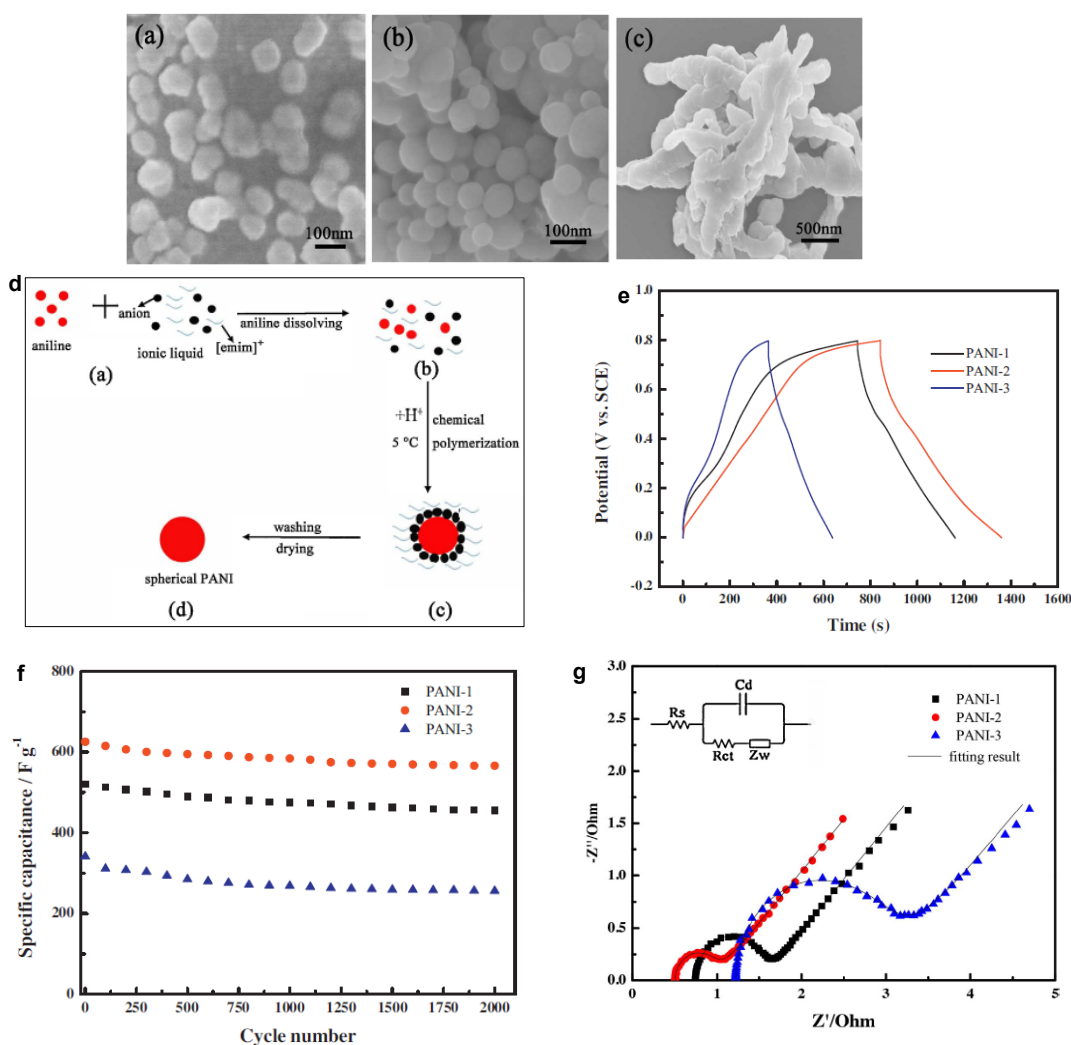
### 3.2.3 AIL anions

The influence of AIL anions on the morphology and electrochemical performances of PANI was investigated in the work completed by Li *et al.* [16]. They prepared PANI in disubstituted imidazolium-based AIL with different anions (*i.e.* 1-ethyl-3-methylimidazolium bromide ((emim)Br) or 1-ethyl-3-methylimidazolium tetrafluoroborate ((emim)BF<sub>4</sub>) via chemical polymerization. The Br<sup>-</sup> and BF<sub>4</sub><sup>-</sup> anions are both hydrophilic but BF<sub>4</sub><sup>-</sup> is less hydrophilic than Br<sup>-</sup> [16]. PANI-1, PANI-2, or PANI-3 are the abbreviates given to PANI prepared in (emim)Br, (emim)BF<sub>4</sub>, or water, respectively. The morphology of the obtained PANI, determined by field emission scanning electron microscopy FESEM, is shown in **Fig. 3**. Uniform spherical PANI particles were obtained in AIL (PANI-1 and PANI-2) instead of random stacking nano-cudgel morphology of PANI prepared in water (PANI-3). In other words, these investigated ionic liquids trigger the formation of PANI with spherical morphology through the arrangement of their ions during polymerization as shown in the schematic process of **Fig. 3d**. While the anions of ionic liquids adsorbed on the surface of PANI, the cations moved to the outer layer. This arrangement induced the formation of spherical PANI. In the role of the

anions in the arrangement of PANI particles, replacing  $\text{Br}^-$  by  $\text{BF}_4^-$  anion decreased the size of PANI particles from 100–120 nm (for PANI-1) to 50–80 nm (for PANI-2), due to less hydrophilic of  $\text{BF}_4^-$  [16].

The electrochemical properties of the three different PANIs were characterized in the three-electrode system in 6 mol/l of KOH using a platinum sheet as a counter electrode and a saturated calomel electrode (SCE) as a reference electrode. The working electrode was titanium mesh (1 x 1 cm) loaded with active material (PANI: acetylene black: polyvinylidene fluoride in a ratio of 85:10:5). **Fig. 3e** shows the charge/discharge curves of all obtained PANI electrode materials from 0 to 0.8 V at 0.1 A/g. These electrodes had capacitive behavior and excellent reversibility as their potential responses were nearly triangle shape during the charge and discharge process. The specific capacitance and capacitance retention over 2000 cycles which are calculated from galvanostatic charge/discharge curves (0 - 0.8 V) at 0.1 A/g and shows in **Fig. 3f**, are as follows: PANI-2 (625 F/g and 90.5 %) > PANI-1 (520 F/g and 87.5 %) > PANI-3 (342 F/g and 75 %). The improvement of capacitance retention observed for PANI-2 owed to its small size particles and its uniform structure. The Nyquist plot in **Fig. 3g**, confirmed the influence of the size of PANI particles on their electrochemical performances. The solution resistances ( $R_s$ ) are 0.75, 0.53 and 1.22  $\Omega$  for PANI-1, PANI-2, and PANI-3, respectively. Moreover, the charge transfer resistance of PANI-2 electrode ( $R_{ct} = 0.55 \Omega$ ) and the PANI-1 sample ( $R_{ct} = 0.89 \Omega$ ) are much lower than that of PANI-3 electrode ( $R_{ct} = 2.04 \Omega$ ). The ion diffusion coefficient in the electrolyte to the electrode surface, (the  $45^\circ$  portion of the curve), is  $6.16 \times 10^{-5}$ ,  $8.58 \times 10^{-5}$ , and  $9.75 \times 10^{-6} \text{ cm}^2/\text{s}$  for PANI-1, PANI-2, and PANI-3, respectively. These parameters indicated that the PANI-2 electrode has better capacitive behaviors than PANI-1.

PANI with small size particles shortens the charge transport distance in the PANI materials and decreases the contact resistance between electrolyte-electrode interfaces [16,33]. Therefore, the counterions of electrolyte easily penetrated the inner layer of PANI to improve charge transfer by the nearly full use of the electrode materials [16, 33].

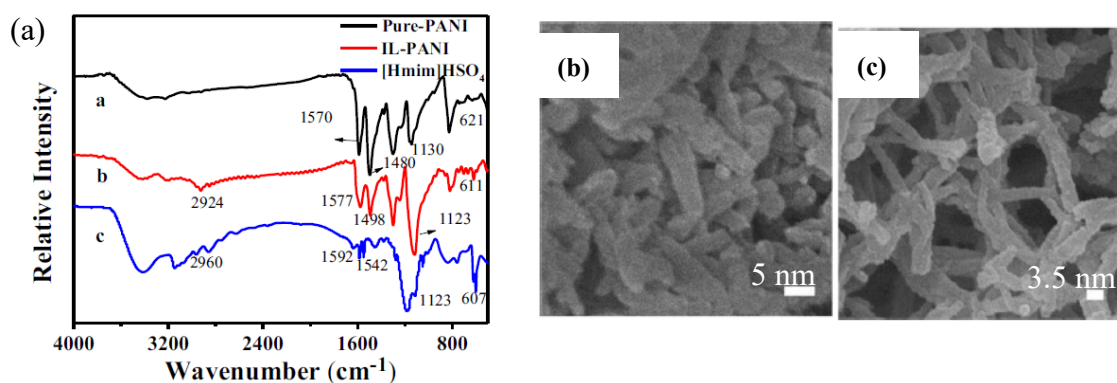


**Fig. 3.** FESEM images of PANI-1 (a), PANI-2 (b) and PANI-3 (c); Schematic formation process of PANI-1 and PANI-2 (d), galvanostatic charge/discharge curves (e), capacitance retention at 0.1 A/g in KOH 6 mol/L (f) and Nyquist plot (g) for PANI-1, PANI-2 and PANI-3 (data is adapted from Ref. [16], Copyright 2014, Elsevier Ltd)

### 3.3 PILs chemical structure

1-methylimidazolium hydrogen sulfate (Hmim)HSO<sub>4</sub> was investigated as a polymerization medium for PANI [46]. PIL has the properties of both Bronsted and Lewis acid in the form of imidazolium ions and hydrogen ions. Therefore, it interacts with the imine structures of PANI via a hydrogen bond [46]. IL-PANI was prepared from aniline in (Hmim)HSO<sub>4</sub> using 1-methyl-3-nbutylimidazopersulfate ((C<sub>4</sub>mim)<sub>2</sub>S<sub>2</sub>O<sub>8</sub>) as an oxidant agent [46]. The structure of IL-PANI was studied by FT-IR spectroscopy whose spectra are shown in **Fig. 4a**. The FT-IR spectrum of IL-PANI showed a certain chemical shift to the right as compared with pure PANI. This indicates that IL-PANI was doped with (Hmim)HSO<sub>4</sub>. The morphology of IL-PANI was compared with that of the conventional PANI. Its SEM images are presented in **Fig. 4b and c**. (Hmim)HSO<sub>4</sub> induced the formation of PANI with porous morphology. The porosity of IL-PANI is related to the molar ratio of aniline to the initiator (C<sub>4</sub>mim)<sub>2</sub>S<sub>2</sub>O<sub>8</sub>. The main issue is the need to prepare (C<sub>4</sub>mim)<sub>2</sub>S<sub>2</sub>O<sub>8</sub> in two steps and to adjust the ratio of (C<sub>4</sub>mim)<sub>2</sub>S<sub>2</sub>O<sub>8</sub> to aniline monomer.

In order to reduce the steps of the PANI polymerization process, (Hmim)HSO<sub>4</sub> and (C<sub>4</sub>mim)<sub>2</sub>S<sub>2</sub>O<sub>8</sub> were replaced by (Pyr)<sub>2</sub>HSO<sub>4</sub> and ammonium peroxydisulfate, respectively [74]. Fiber-like morphology of PANI/PIL was obtained instead of agglomerated morphology of the conventional PANI. The specific capacitance, calculated from galvanostatic charge/discharge curves, was 173 and 63 F/g at 10 A/g for PANI/PIL and conventional PANI, respectively. The enhancement of specific capacitance was contributed to by its nanostructured and fibrillary morphology. The electrochemical performances of PANI/PIL and the conventional PANI were studied in H<sub>2</sub>SO<sub>4</sub> 1 mol/L using a symmetrical two-electrode system configuration [74].



**Fig. 4.** (a) FTIR spectra of Pure PANI, IL-PANI, and (Hmim)HSO<sub>4</sub>, SEM images of (b) pure PANI and (c) IL-PANI (data id from Ref. [46], Copyright 2019, Springer Nature Switzerland AG)

In summary, ionic liquids as a polymerization medium dope PANI chains [46,72] or are easily removed during the purification of PANI according to their chemical structure [16,35,74]. Ionic liquids play the role of a soft template agent and promote the formation of well-defined one-dimensional morphology of PANI that have a positive influence on the electrochemical behaviors. Other ionic liquids induce the formation of lamellar particles which is detrimental to the electrochemical performances of PANI. The choice of ionic liquids is a key to control the morphology of PANI and its related properties.

## 4. Ionic liquids as electrolyte for PANI electrodes

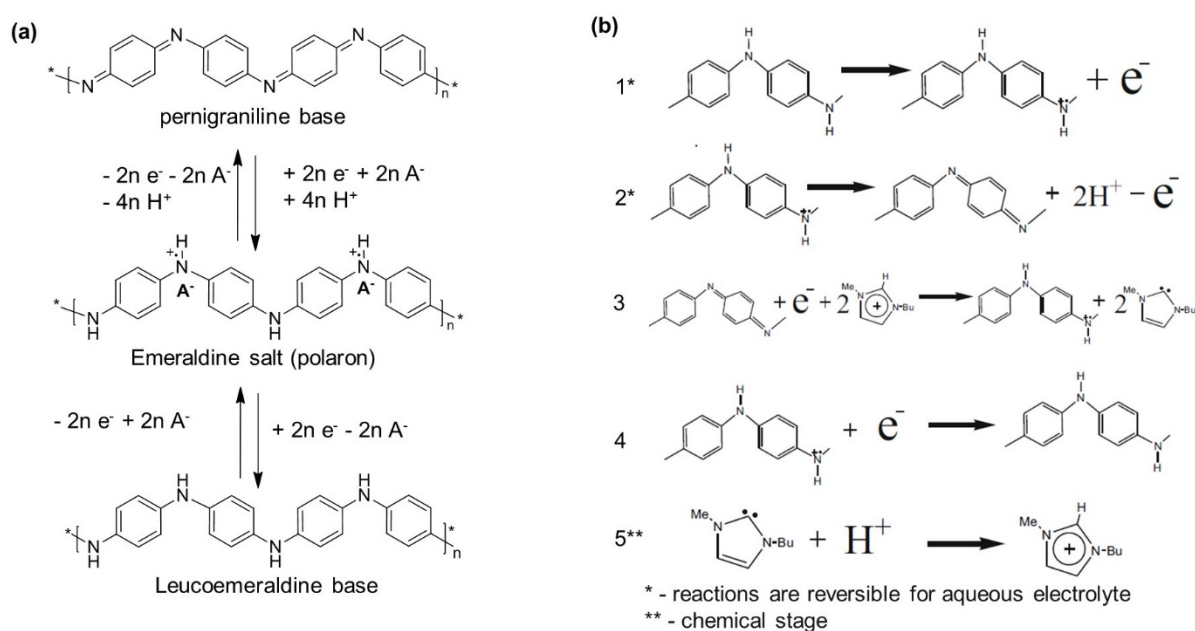
The electrochemical performances of PANI are strongly related to the electrolyte in which it is characterized. The electrolytes are classified into four categories as follows [76].

- **Conventional aqueous acid electrolytes** are characterized by their good ionic concentration, low resistance, and high ionic conductivity. However, they have a limited operating potential window (upto 1 V).
- **Organic electrolytes** in a mixture with conducting salts (*e.g.* tetraethylammonium tetrafluoroborate/propylene carbonate) have commonly been used in commercially available EDLCs. Organic electrolytes provide a wider electrochemical window than aqueous acid electrolytes. On the other side, its toxicity, volatility, and flammability are real issues.
- **Gel polymer** has been introduced with a low cost and nontoxicity. However, it has low ionic conductivity and inferior interfacial properties with electrodes at low temperatures as well as at room temperature [23,76,77].
- **Ionic liquid-based electrolytes** have received considerable attention owing to their properties: low vapor pressure, thermal and chemical stability, high ionic conductivity, and non-inflammability. These properties label them a ‘green electrolyte’. They are also characterized by the wide electrochemical stability window (~3.5–5V) and well-defined ion size [47,78–85].



In conventional aqueous acid electrolytes, PANI electrodes display two coupled peaks on CV curves and attribute to the redox transformation of PANI between different oxidation states [25,86]. **Fig. 5a** summarizes the two redox processes of PANI as described in the literature [28]. The first one corresponds to the reversible transformation between the leucoemeraldine base (fully reduced form of PANI) and emeraldine salt forms (partially oxidized form) [28]. It involves electron transfer only. In other words, the oxidation of the leucoemeraldine base to the emeraldine salt means that an electron is lost per a dimer aniline rings in PANI, which is positively charged. Hence, the electroneutrality of PANI is maintained by the diffusion of counterion from electrolytes to the PANI surface [33]. The counterion diffusion into/out of the polymer is related to PANI morphology, and the diffusion is the best in the case of PANI with nanostructured morphology and the regular shape of nanoparticles [33]. The second redox process is associated to the emeraldine/pernigraniline (*i.e.* fully oxidized form) couple. It involves not only electron transfer but also proton transfer [28]. PANI exhibits destruction of its chains during cycle life tests in conventional aqueous acid electrolytes for the following two basic reasons [28-31,33].

- PANI electrode is affected by swelling-shrinking during counterion influx and outflux from the polymer
- Pernigraniline is easily hydrolyzed because of its imine group



**Fig. 5.** Reactions of PANI transformation in conventional aqueous electrolytes (a) and AILs/acetonitrile electrolytes (b) (a is from the reference [28], copyright 2013, the Owner Societies and b from Ref. [87], copyright 2020, Springer-Verlag GmbH Germany, part of Springer Nature)

Ionic liquids have recently been investigated in terms of their properties as electrolytes for PANI improves the cycle life stability of PANI [33,40,44,53,87]. Generally, PANI electrodes have displayed low but stable specific capacitance in “neat” ionic liquids. Innis et al. showed that PANI film exhibited a stable specific capacitance over 100 cycles in 1-ethyl-3-methylimidazolium bis(trifluoromethanesulfonyl)imide (EMITFSI) electrolyte while it was degraded with 30 cycles in propylene carbonate (organic electrolyte) [40]. The characterization was carried out by using cyclic voltammetry between -0.4 and 1.5 V with a scan rate of 100 mV [40]. Similarly, Wang et al. presented that PANI capacitance almost had no decrease in EMITFSI vs. 12 % loss in HClO<sub>4</sub> 1 mol/l (aqueous electrolyte) after 500 cycles at 20 A/g [33]. The stable electrochemical response of PANI in neat EMITFSI was obtained by the intrinsic stability and wide electrochemical window of EMITFSI where no side reaction happened. On the contrary, the specific capacitance of PANI in EMITFSI was the lowest compared with that obtained in an aqueous electrolyte. For instance, the specific capacitance of PANI in EMITFSI (~280 F/g at 20 A/g) was almost two times lower than that obtained in HClO<sub>4</sub> (~780 F/g) [33]. That difference was caused by the low ionic conductivity and high viscosity of neat EMITFSI compared to HClO<sub>4</sub> [33].

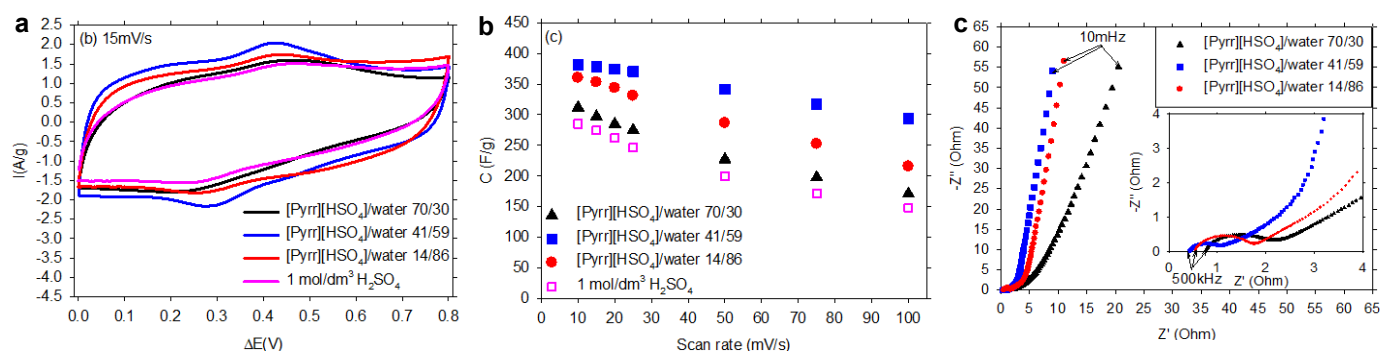
Binary mixtures of AILs/organic solvents were used as an alternative to “neat” ionic liquids because they experience better transport properties (lower viscosity and higher ionic conductivity than “neat” ionic liquids) [44,87]. A comparative study of the electrochemical performances of PANI film in neat 1-methyl-3-butylimidazolium hexafluorophosphate (BMIPF6) and binary mixture acetonitrile/BMIPF6 with different volume ratios (25/75, 50/50, and 75/25) was carried out by Ling et al. [44]. The specific capacitance of PANI was higher in acetonitrile/BMIPF6 than that obtained in neat BMIPF6. The specific capacitance was around

19.1 mF/cm<sup>2</sup> in neat BMIPF6 and gradually rose to 72.6 mF/cm<sup>2</sup> in acetonitrile/BMIPF6 of a volume ratio of 75/25. These values were calculated from galvanostatic discharge curves in a three-electrode system at 0.1 mA/cm<sup>2</sup> in the voltage range of 0–1 V. The specific capacitance values of PANI showed a similar trend with the ionic conductivity of binary mixture acetonitrile/BMIPF6. The ionic conductivity value was 2.3 mS/cm for neat BMIPF6 and progressively increased with the addition of acetonitrile till reached 78.8 mS/cm for acetonitrile/BMIPF6 of a volume ratio of 75/25. The specific capacitance of PANI was improved along with the addition of acetonitrile into BMIPF6 because the anions were solvated before insertion into the polymer [44]. Despite the enhancement, the electroactivity of PANI dropped during the first 300 cycles. This loss was explained by the fact that the redox transformations of PANI were not completely reversible in AILs/acetonitrile. The detailed mechanism of redox processes of PANI, as described by Lebedeva *et al.* [87].

**Fig. 5b** depicts that the transformation of emeraldine-leucoemeraldine is the same as in conventional aqueous acid electrolyte (**Fig. 5b**). In contrast, the transformation requires the involvement of AILs cation. 1-butyl-3-methylimidazolium BMIM<sup>+</sup> ion, which interacts with imine groups of pernigraniline was considered a source of proton necessary for pernigraniline reduction with emeraldine formation (**Fig. 5b**, equation 3). Deprotonation of BMIM<sup>+</sup> results in the formation of a carbene, which, in its turn, reacts chemically in the bulk of electrolyte with protons forming BMIM<sup>+</sup> cation (**Fig. 5b**).

On the other hand, PILs/water (*i.e.* pyrrolidinium hydrogen sulfate (Pyrr)(HSO<sub>4</sub>)/water) were also used as electrolytes for PANI since aqueous electrolytes are environmentally friendly and safety solvents. Additionally, PANI is electroactive in acidic media [43]. (Pyrr)HSO<sub>4</sub> is a PIL with high proton activity (its equivalent pH is 1.9) and identified as a suitable electrolyte for electropolymerization of PANI [53]. The electrochemical measurements were carried out in a symmetrical two-electrode system with three different (Pyrr)HSO<sub>4</sub>/water weight ratios. The electrodes were prepared by pressing 3 mg of the paste containing 60 wt% of PANI, 32 wt% of carbon black, and 8 wt% of PTFE on stainless steel mesh with a diameter of 0.8 cm. **Fig. 6a** presents the obtained CV curves of PANI in (Pyrr)HSO<sub>4</sub>/water weight ratio *c.a.* 14/86, 41/59, or 70/30 as well as in H<sub>2</sub>SO<sub>4</sub> 1 mol/l. All CV curves displayed the redox peaks of PANI that contributed to the transformation between leucoemeraldine and emeraldine. The highest area of the CV curve, however, was obtained in the ratio of 41/59 of (Pyrr)HSO<sub>4</sub>/water, compared to the other selected electrolytes (H<sub>2</sub>SO<sub>4</sub> 1 mol/l). The specific capacitance values of the PANI single electrode, calculated from CV curves, are presented in **Fig. 6b**. The specific capacitance values of PANI in (Pyrr)HSO<sub>4</sub>/water were higher than that obtained in H<sub>2</sub>SO<sub>4</sub> at all selected scan rates and regardless of the weight ratio. Furthermore, similarly to what was observed in acetonitrile/BMIPF6, PANI-specific capacitance followed the same order of the electrolyte ionic conductivity. For instance, the higher specific capacitance of PANI was obtained in the ratio of 41/59 of (Pyrr)HSO<sub>4</sub>/water with the optimum ionic conductivity. The dependence of PANI electrochemical performances on ionic conductivity of the (Pyrr)HSO<sub>4</sub>/water ratio was also confirmed by the Nyquist plot shown in **Fig. 6c**. The ionic resistance (R<sub>s</sub>), evaluated from the intercept of the Nyquist plot with the real axis, was 0.43, 0.56, and 0.78 Ω in the weight ratio of 41/59, 14/86, and 70/30 of (Pyrr)HSO<sub>4</sub>/water, respectively. The order of obtained R<sub>s</sub> values is opposite to that of the electrolyte ionic conductivity. Moreover, PANI electrodes displayed the lowest transport resistance (evaluated from semi-circle diameter) in the ratio of 41/59 of (Pyrr)HSO<sub>4</sub>/water and showed good interaction with electrode–electrolyte. Additionally, the faster ions diffusion was also obtained as a line nearly parallel to the imaginary axis in this electrolyte. The retention of the specific capacitance of PANI was about 68 % over 1000 cycles, which is better than that reported with the conventional electrolyte of 1 mol/dm<sup>3</sup> H<sub>2</sub>SO<sub>4</sub> [43]. Although the improvement in the capacitance retention of PANI in the mixture of (Pyrr)HSO<sub>4</sub> and water, the cycle life stability is not yet enough.

Concerning the charge storage mechanism in PILs, there is no need for the contribution of the cation of the ionic liquid as they have excess proton as opposite to the proposed mechanism in acetonitrile/BMIPF6. The mechanism of proton conduction (Grotthuss or vehicle mechanism) in PILs/water is related to its ionic transport properties [88,89]. A combination of the Grotthuss mechanism (*i.e.* the protons are passed along hydrogen bonds) and vehicle mechanism (*i.e.* the proton movement occurs with the aid of a moving “vehicle” such as H<sub>2</sub>O or Imidazole) exists in PILs/water mixture [43]. However, the Grotthuss mechanism is dominant in viscous PILs [43,88].

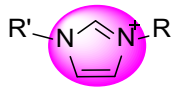
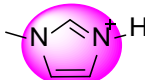

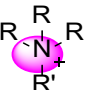



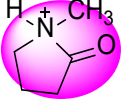
**Fig. 6.** (a) CV curves at 15 mV/s, (b) specific capacitance as a function of scan rate and (c) Nyquist plots at open circuit potential between 10 mHz and 500 kHz (shown more clearly in the inset) of PANI in the weight ratio of 70/30, 41/59, and 14/86 of (Pyrr)HSO<sub>4</sub>/water in H<sub>2</sub>SO<sub>4</sub> 1 mol/L (data is from Ref. [43]. Copyright 2019, Elsevier B. V).

### 5. List of used ionic liquids for PANI

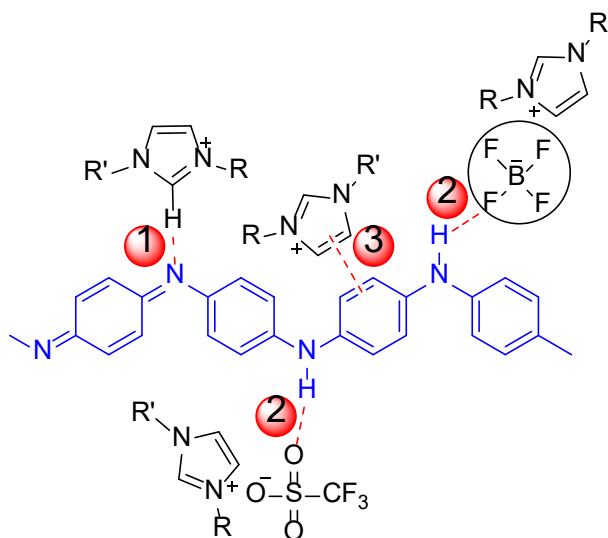
There are various ionic liquids used for the preparation or electrochemical characterization of PANI. **Table 3** summarizes the cation structures as well as the full and abbreviated names of ionic liquids used in the literature for PANI. **Table 3** shows that ionic liquids with different chemical structures (cations, anions, and alkyl groups) were used. The most used ionic liquids are aprotic and especially 1,3-dialkylimidazolium-based AILs.

**Table 3.** Cation structures, full names, abbreviated names and role of investigated ionic liquids for PANI material

Cation structures	ionic liquid names	Abbreviated names	use	Ref
 1,3-disubstituted imidazolium	1-ethyl-3-methylimidazolium tetrafluoroborate or bromide	(emim)BF <sub>4</sub> or (emim)Br	solvent	[16]
	1-alkyl-3-methylimidazolium chloride; Alkyl: methyl-, ethyl-, butyl-, octyl-, decyl- and hexadecyl-	(RMeIm)Cl	additive into solvent	[35]
	1-butyl-3-methylimidazolium chloride	(bmim)Cl	additive into solvent	[34]
	1,3-dimethyl imidazolium methyl sulfate	(Me <sub>2</sub> Im)MeOSO <sub>3</sub>	solvent	[35]
	1-ethyl-3-methylimidazolium trifluoromethanesulfonate		dopant	[38]
	1-butyl-3-methylimidazolium hexafluorophosphate	BMIPF <sub>6</sub>	Electropolymerization medium	[51]
			electrolyte	[44]
	1-ethyl-3-methylimidazolium bis(trifluoromethane sulfonyl)imide	EMITFSI	electrolyte	[33, 40]
 1-methylimidazolium	1-butyl-3-methylimidazolium tetrafluoroborate or hexafluorophosphate	(BMIM)BF <sub>4</sub> or (BMIM)PF <sub>6</sub>	electrolyte	[41, 87]
	1-ethylacetate-3-methylimidazolium tetrafluoroborate	(EAMIM)BF <sub>4</sub>	Solvent	[75]
	1-alkyl-3-carboxymethyl imidazolium chloride; Alkyl: methyl, vinyl, allyl, butyl, hexyl	(RCMIm)Cl	solvent	[72]
	1-methylimidazolium hydrogen sulfate	(Hmim)HSO <sub>4</sub>	solvent and dopant	[46]
 1,4-dialkylpyridinium	1-butyl-4-methylpyridinium chloride	(BuMePyr)Cl	additive into solvent	[35]
	methyltributylammonium chloride	(Bu <sub>3</sub> MeN)Cl	additive into solvent	[35]
 tetraalkylammonium	2-hydroxyethylammonium formate		solvent	[42]
	Ethylammonium nitrate	EAN	electropolymerization medium	[45]

 pyrrolidinium	1-butyl-1-methylpyrrolidinium bis (trifluoromethanesulfonyl)imide	C <sub>4</sub> mpyrTFSI	electropolymerization medium	[45]
	pyrrolidinium hydrogen sulfate	(Pyr)HSO <sub>4</sub>	electrolyte	[43, 53]
			solvent	[74]
			electropolymerization medium	[53]
	Pyrrolidinium nitrate	(Pyr)NO <sub>3</sub>	Electropolymerization medium	[53]
 1-methyl-2-pyrrolidonium	1-methyl-2-pyrrolidonium hydrogen sulfate	(NMP)HSO <sub>4</sub>	Electropolymerization medium	[52]

According to Refs. [35,37,38,46,90], 1,3-dialkylimidazolium-based AILs interacts with PANI through non-covalent interactions as shown in **Fig. 7**. First of all, the hydrogen atom in the 2-position of imidazolium (sufficiently acid) have hydrogen bonding interactions with imine nitrogen of PANI [38], indicated as number 1 in **Fig. 7**. Furthermore, the formation of the hydrogen bond is also possible between the secondary amino group of PANI and the anionic part of AIL (*e. g.* tetrafluoroborate (BF<sub>4</sub><sup>-</sup>) or trifluoromethanesulfonate (CF<sub>3</sub>SO<sub>3</sub><sup>-</sup>)) [37,38], presented as number 2 in **Fig. 7**. Hydrogen bond acts as a cross-linking agent, which is beneficial for polymer properties (*e.g.* mechanical properties, thermostability) [91]. As for PANI, hydrogen bond cross-linking reduces the interlayer spacing between PANI chains and induces the formation of porous morphology [46]. The third possible non-covalent interaction is  $\pi$ - $\pi$  interactions between imidazolium nuclei and PANI [90,92] (number 3 in **Fig. 7**). The non-covalent interactions between PANI and ionic liquids provide the role of ionic liquids as a soft template agent, and therefore, the interactions induce the organization of PANI chains in solutions and the formation of nanostructured PANI morphology via homogeneous nucleation.



**Fig. 7.** Possible interactions between PANI and AIL: (1) hydrogen bond between imine nitrogen of PANI and hydrogen atom in the 2-position of imidazolium, (2) hydrogen bond between secondary amino group in PANI and anion of AIL and (3)  $\pi$ - $\pi$  interaction between PANI and 1,3-dialkylimidazolium cation

## 6. Conclusions

The combination of ionic liquids with PANI has been recently investigated for supercapacitor applications and shown the following results:

- As a polymerization medium, ionic liquids lead to the formation of green-conducting nanostructured PANI salt (emeraldine form) with a uniform shape instead of agglomerated granular morphology of conventional PANI. The one-dimensional nanostructured PANI electrodes have shown an improvement in charge transfer by reducing the contact resistance between electrode-electrolyte interfaces, when compared to the conventional PANI. The role of ionic liquids as a soft template has been



strongly related to its compositions (alkyl chain length, head group structure, anions) as well as to the aniline/ionic liquid mole ratio.

- As electrolytes, the efficiency of ionic liquids is related to their transport properties (viscosity, ionic conductivity). In neat AILs, PANI electrodes exhibited stable cycle life but low specific capacitance due to the high viscosity and low ionic conductivity of the neat ionic liquids. The electrochemical properties of PANI in acetonitrile/BMIPF6 with different volume ratios and (Pyrr)HSO<sub>4</sub>/water ratios were strongly related to the ionic conductivity of the investigated electrolytes. The best specific capacitance of PANI was obtained in the volume ratio of 75/25 of acetonitrile/BMIPF6 or the weight ratio of 41/59 of (Pyrr)HSO<sub>4</sub>/water, which have the optimal ionic conductivity as compared to the other formulations. Ionic liquids/solvents as the electrolyte for PANI electrodes are promising and a good alternative to the conventional aqueous electrolytes (H<sub>2</sub>SO<sub>4</sub>, HCl) in terms of specific capacitance and diffusion resistance.
- Concerning the electropolymerization of aniline, as opposite to AILs which require the addition of an exogenous proton source, PILs with protonated anion (*e.g.* (NMP)HSO<sub>4</sub> or (Pyrr)HSO<sub>4</sub>) are convenient to prepare PANI film of high quality.
- 1,3-dialkylimidazolium-based AILs have been the most used ionic liquids for PANI owing to the possible non-covalent interactions between AILs and PANI. However, they do not have excess protons, which are key to a fast rate for PANI polymerization. In contrast, imidazolium-based PIL is not frequently used although it has the properties of both Bronsted and Lewis acid.
- PILs have been used for PANI synthesis or electrochemical studies although they present enough excess protons owing to their labile hydrogen.
- Synthesis and electrochemical characterization of PANI in ionic liquids are more promising than preparing PANI in ionic liquids and its electrochemical behaviors in conventional electrolytes or vice-versa. This approach is not fully investigated.

The combination of ionic liquids with PANI provides an effective approach to resolve the lack of cycle life stability of PANI. Not all ionic liquids are appropriate for preparation (by electrodeposition or oxidative polymerization) or electrochemical characterization of PANI. Thus, the choice of ionic liquid types or structures is the key to the desired outcomes.

**Funding:** This research did not receive external funding

**Acknowledgments:** We would like to acknowledge Dr. Martial Degbia from IKAMBA Organics laboratory, Dr. Bruno Schmaltz and Dr. Fouad Ghamouss from university of Tours, Dr. Khlalil Cherry from the Lebanese university for the helpful discussion.

## References

1. Tecate Group Home Page. Available online: [www.tecategroup.com](http://www.tecategroup.com). (accessed on February 10, 2022)
2. Maxwell Home page. Available online: [www.maxwell.com](http://www.maxwell.com). (accessed on February 10, 2022)
3. Skeleton technology Home Page. Available online: [www.skeletontech.com](http://www.skeletontech.com). (accessed on February 10, 2022)
4. Yu, L.; Chen, G.Z. Supercapattories as High-Performance Electrochemical Energy Storage Devices. *Electrochemical Energy Reviews*. **2020**, *3*:271–85.
5. Numan, A.; Zhan, Y.; Khalid, M.; Hatamvand, M.; Arshid, N.; Grace, A.N. Chapter three - Introduction to supercapattery. *Advances in Supercapacitor and Supercapattery*: Elsevier 2021:45-61.
6. Iro ZS, Subramani C, Dash SS. A Brief Review on Electrode Materials for Supercapacitor. *Int J Electrochem Sci*. **2016**, *11*:10628-43.
7. Wang, G.; Zhang, L.; Zhang, J. A review of electrode materials for electrochemical supercapacitors. *Chem Soc Rev*. **2012**, *41*:797–828.
8. Wu, Z., Zhang, X.-B. Design and Preparation of Electrode Materials for Supercapacitors with High Specific Capacitance. *Acta Phys Chim Sin*. **2017**, *33*:305–13.
9. Jiang, J; Zhang, Y.; Nie, P.; Xu, G.; Shi, M.; Wang, J. et al. Progress of Nanostructured Electrode Materials for Supercapacitors. *Adv Sustain Syst*. **2017**, *2*:1700110.
10. Samantara, A.K.; Ratha, S. Materials Development for Active/Passive Components of a Supercapacitor. 2017.
11. Mishra, M. Encyclopedia of polymer application. 2018:991.
12. Snook, G.A., Kao, P.; Best, A.S. Conducting-polymer-based supercapacitor devices and electrodes. *J Power Sources*. **2010**, *196*:1–12.
13. Beguin, F.; Frackowiak, E. *Supercapacitors: Materials, Systems, and Applications*. 2013.
14. Eaton Supercapacitors Home Page. Available online: <https://www.eaton.com/us/en-us/products/electronic-components/faq/what-is-a-hybrid-supercapacitor.html>. (accessed on February 10, 2022)
15. Veerasubramani, G.K.; Krishnamoorthy, K.; Radhakrishnan, S.; Kim, N.-J., Kim, S.-J. In-situ chemical oxidative polymerization of aniline monomer in the presence of cobalt molybdate for supercapacitor applications. *J Ind Eng Chem* **2016**, *36*:163–8.
16. Li, X.; Liu, Y.; Guo, W.; Chen, J.; He, W.; Peng, F. Synthesis of spherical PANI particles via chemical polymerization in ionic liquid for high-performance supercapacitors. *Electrochim Acta* **2014**, *135*:550–7.

17. Chellachamy Anbalagan A, Sawant, S.N. Brine solution-driven synthesis of porous polyaniline for supercapacitor electrode application. *Polymer*. **2016**, *87*:129–37.
18. Bhandari, S.; Khastgir, D. Template-free solid state synthesis of ultra-long hairy polyaniline nanowire supercapacitor. *Mater Lett*. **2014**, *135*:202–5.
19. Gholivand, M.B.; Heydari, H.; Abdolmaleki, A.; Hosseini, H. Nanostructured CuO/PANI composite as supercapacitor electrode material. *Mater Sci Semicond Process*. **2015**, *30*:157–61.
20. Wang, X.; Liu, D.; Deng, J.; Duan, X.; Guo, J.; Liu, P. Improving cyclic stability of polyaniline by thermal crosslinking as electrode material for supercapacitors. *RSC Adv*. **2015**, *5*:78545–52.
21. Khadry, N.H., Abdesalam, M.E.; Enany G. Mesoporous Polyaniline Films for High Performance Supercapacitors. *J Electrochem Soc*. **2014**, *161*:G63–G8.
22. Ramya, R.; Sivasubramanian, R; Sangaranarayanan, M.V. Conducting polymers-based electrochemical supercapacitors-Progress and prospects. *Electrochim Acta*. **2013**, *101*:109–29.
23. Bhadra, S.; Khastgir, D.; Singha, N.K.; Lee, J.H. Progress in preparation, processing and applications of polyaniline. *Prog Polym Sci*. **2009**, *34*:783–810.
24. Pauliukaite, R.; Brett, C.M.A; Monkman, A.P. Polyaniline fibres as electrodes.: Electrochemical characterisation in acid solutions. *Electrochim Acta*. **2004**, *50*:159–67.
25. Huang, W.S.; Humphrey, B.D.; MacDiarmid, A.G. Polyaniline, a novel conducting polymer. Morphology and chemistry of its oxidation and reduction in aqueous electrolytes. *J Chem Soc, Faraday Trans 1*. **1986**, *82*:2385–400.
26. Chaudhari, S.; Sharma, Y.; Archana, P.S.; Jose, R.; Ramakrishna, S.; Mhaisalkar, S. et al. Electrospun polyaniline nanofibers web electrodes for supercapacitors. *J Appl Polym Sci*. **2013**, *129*:1660–8.
27. Prakash, R. Electrochemistry of polyaniline: Study of the pH effect and electrochromism. *J Appl Polym Sci*. **2002**, *83*:378–85.
28. Jeon, J.-W.; Ma, Y.; Mike, J.F.; Shao, L.; Balbuena, P.B.; Lutkenhaus, J.L. Oxidatively stable polyaniline:polyacid electrodes for electrochemical energy storage. *Phys Chem Chem Phys*. **2013**, *15*:9654–62.
29. Li, Z.-F.; Zhang, H.; Liu, Q.; Liu, Y.; Stanciu, L.; Xie, J. Covalently-grafted polyaniline on graphene oxide sheets for high performance electrochemical supercapacitors. *Carbon*. **2014**, *71*:257–67.
30. Cong, H.-P.; Ren, X.-C.; Wang, P.; Yu, S.-H. Flexible graphene-polyaniline composite paper for high-performance supercapacitor. *Energy Environ Sci*. **2013**, *6*:1185–91.
31. Cui, Q.; Mi, H.; Qiu, J.; Yu, C.; Zhao, Z. Interconnected polyaniline clusters constructed from nanowires: Confined polymerization and electrochemical properties. *J Mater Res*. **2014**, *29*:2408–15.
32. Gao, H.; Jiang, T.; Han, B.; Wang, Y.; Du, J.; Liu, Z. et al. Aqueous/ionic liquid interfacial polymerization for preparing polyaniline nanoparticles. *Polymer*. **2004**, *45*:3017–9.
33. Wang, K.; Huang, J.; Wei, Z. Conducting Polyaniline Nanowire Arrays for High Performance Supercapacitors. *J Phys Chem C*. **2010**, *114*:8062–7.
34. Pahovnik D, Žagar E, Vohlidal J, Žigon M. Ionic liquid-induced formation of polyaniline nanostructures during the chemical polymerization of aniline in an acidic aqueous medium. *Synth Met*. **2010**, *160*:1761–6.
35. Pahovnik, D.; Žagar, E.; Kogej, K.; Vohlidal, J.; Žigon, M. Polyaniline nanostructures prepared in acidic aqueous solutions of ionic liquids acting as soft templates. *Eur Polym J*. **2013**, *49*:1381–90.
36. Krishna, A.; Laslau, C.; Waterhouse, G.; Zujovic, Z.; Travas-Sejdic J. Effect of ionic liquid on polyaniline chemically synthesised under falling-pH conditions. *Chemical Papers*. **2013**, *67*:995–1001.
37. Yang, D.; Fadeev, A.G.; Adams, P.N.; Mattes, B.R. GPC characterization of emeraldine base in NMP containing ionic liquids. *Synth Met*. **2007**, *157*:988–96.
38. Stejskal, J.; Dybal, J.; Trchova, M. The material combining conducting polymer and ionic liquid: Hydrogen bonding interactions between polyaniline and imidazolium salt. *Synth Met*. **2014**, *197*:168–74.
39. Miao, Z.; Wang, Y.; Liu, Z.; Huang, J.; Han, B.; Sun, Z. et al. Synthesis of polyaniline nanofibrous networks with the aid of an amphiphilic ionic liquid. *J Nanosci Nanotechnol*. **2006**, *6*:227–30.
40. Innis, P.C.; Mazurkiewicz, J.; Nguyen, T.; Wallace, G.; MacFarlane, D. Enhanced electrochemical stability of polyaniline in ionic liquids. *Curr Appl Phys*. **2004**, *4*:389–93.
41. Lu, W.; Fadeev, A.G.; Qi, B.; Smela, E.; Mattes, B.R., Ding, J. et al. Use of ionic liquids for pi-conjugated polymer electrochemical devices. *Science*. **2002**, *297*:983–7.
42. Bicak, N.; Senkal, B.F.; Sezer, E. Preparation of organo-soluble polyanilines in ionic liquid. *Synth Met*. **2005**, *155*:105–9.
43. Al-Zohbi, F.; Jacquemin, J.; Ghamouss, F.; Schmaltz, B.; Abarbri, M.; Cherry, K. et al. Impact of the aqueous pyrrolidinium hydrogen sulfate electrolyte formulation on transport properties and electrochemical performances for polyaniline-based supercapacitor. *J Power Sources*. **2019**, *431*:162–9.

44. Ling Zang, J.-L.; Zang, X.-G.; Xiao, F.; H, F.-P. Effect of polar solvent acetonitrile on the electrochemical behavior of polyaniline in ionic liquid electrolytes. *J Colloid Interface Sci.* **2005**, *287*:67–71.
45. Snook, G.A.; Greaves, T.L.; Best, A.S. A comparative study of the electrodeposition of polyaniline from a protic ionic liquid, an aprotic ionic liquid and neutral aqueous solution using anilinium nitrate. *J Mater Chem.* **2011**, *21*:7622–9.
46. Li, S.; Yang, C.; Sarwar, S.; Nautiyal A; Zhang P; Du H, et al. Facile synthesis of nanostructured polyaniline in ionic liquids for high solubility and enhanced electrochemical properties. *Adv Compos Hybrid Mater.* **2019**, *2*:279–88.
47. Arbizzani, C.; Biso, M.; Cericola, D.; Lazzari, M.; Soavi, F.; Mastragostino, M. Safe, high-energy supercapacitors based on solvent-free ionic liquid electrolytes. *J Power Sources.* **2008**, *185*:1575-9.
48. Ohno, H. In *Electrochemical Aspects of Ionic Liquids*. Koganei, Tokyo, Japan. 2011.
49. Aranowski, R.; Cichowska-Kopczyńska, I.; Dębski, B.; Jasiński, P. Conductivity and viscosity changes of imidazolium ionic liquids induced by H<sub>2</sub>O and CO<sub>2</sub>. *J Mol Liq.* **2016**, *221*:541–6.
50. Vogl, T.; Goodrich, P.; Jacquemin, J.; Passerini, S.; Balducci, A. The Influence of Cation Structure on the Chemical-Physical Properties of Protic Ionic Liquids. *J Phys Chem C.* **2016**, *120*:8525-33.
51. Wei, D.; Kvarnstrom, C.; Lindfors, T.; Ivaska, A. Polyaniline nanotubes obtained in room-temperature ionic liquids. *Electrochem Commun.* **2006**;8:1563-6.
52. Patil, D.S.; Pawar, S.A.; Patil, S.K.; Salavi, P.P.; Kolekar, S.S.; Devan, R.S. et al. Electrochemical performance of potentiodynamically deposited polyaniline electrodes in ionic liquid. *J Alloys Compd.* **2015**, *646*:1089–95.
53. Shen, L.; Huang, X. Electrochemical polymerization of aniline in a protic ionic liquid with high proton activity. *Synth Met.* **2018**, *245*:18–23.
54. Ismail, H.K.; Alesary, H.F.; Al-Murshedi, AY.M.; Kareem, J.H. Ion and solvent transfer of polyaniline films electrodeposited from deep eutectic solvents via EQCM. *J Solid State Electrochem.* **2019**, *23*:3107–21.
55. Yilmaz Erdogan P.; Zengin, H.; Yavuz, A. Growth and cycling of polyaniline electrode in a deep eutectic solvent: A new electrolyte for supercapacitor applications. *Solid State Ionics.* **2020**, *352*:115362.
56. Naudin, E; Ho, H.A.; Breau, L.; Belanger, D. Electrochemical behavior of polyaniline and polythiophene derivatives in various electrolytes. *ACS Symp Ser.* **2003**, *832*:52–8.
57. Cao, Y.; Andreatta, A.; Heeger, A.J.; Smith, P. Influence of chemical polymerization conditions on the properties of polyaniline. *Polymer.* **1989**, *30*:2305–11.
58. Sapurina, I.Y.; Stejskal, J. Oxidation of aniline with strong and weak oxidants. *Russ J Gen Chem.* **2012**, *82*:256–75.
59. Stejskal, J.; Sapurina, I.; Trchová, M. Polyaniline nanostructures and the role of aniline oligomers in their formation. *Prog Polym Sci.* **2010**, *35*:1420–81.
60. Sapurina, I.; Stejskal, J. The mechanism of the oxidative polymerization of aniline and the formation of supramolecular polyaniline structures. *Polym Int.* **2008**, *57*:1295–325.
61. Kuang, H.; Cao, Q.; Wang, X.; Jing, B.; Wang, Q.; Zhou, L. Influence of the reaction temperature on polyaniline morphology and evaluation of their performance as supercapacitor electrode. *J Appl Polym Sci.* **2013**, *130*:3753–8.
62. Li, D.; Huang, J.; Kaner, R.B. Polyaniline Nanofibers: A Unique Polymer Nanostructure for Versatile Applications. *Acc Chem Res.* **2009**, *42*:135–45.
63. Li, D.; Kaner, R.B. Shape and Aggregation Control of Nanoparticles: Not Shaken, Not Stirred. *J Amer Chem Soc* **2006**, *128*:968–75.
64. Sinha, S.; Bhadra, S.; Khastgir, D. Effect of dopant type on the properties of polyaniline. *J Appl Polym Sci.* **2009**, *112*:3135–40.
65. Paul, R.K.; Pillai, C.K.S. Thermal properties of processable polyaniline with novel sulfonic acid dopants. *Polym Int.* **2001**, *50*:381–6.
66. Stejskal, J.; Gilbert, R.G. Polyaniline. Preparation of a conducting polymer (IUPAC technical report). *Pure Appl Chem.* **2002**, *74*:857–67.
67. Catedral, M.; Tapia, A.K.G.; Sarmago, R.; Tamayo, J.P.; Rosario, E.J.d. Effect of Dopant Ions on the Electrical Conductivity and Microstructure of Polyaniline (Emeraldine Salt). *Science Diliman.* **2004**, *16*: 41-6.
68. Pron, A.; Genoud, F.; Menardo, C.; Nechtschein, M. The effect of the oxidation conditions on the chemical polymerization of polyaniline. *Synth Met.* **1988**, *24*:193–201.
69. Ding, H.; Wan, M.; Wei, Y. Controlling the diameter of polyaniline nanofibers by adjusting the oxidant redox potential. *Adv Mater* **2007**, *19*:465–9.
70. Li K, Guo D, Chen J, Kong Y, Xue H. Oil-water interfacial synthesis of graphene-polyaniline-MnO<sub>2</sub> hybrids using binary oxidant for high performance supercapacitor. *Synth Met.* **2015**, *209*:555–60.
71. Shahzad, S.; Shah, A.; Kowsari, E.; Iftikhar, F.J.; Nawab, A.; Piro, B. et al. Ionic Liquids as Environmentally Benign Electrolytes for High-Performance Supercapacitors. *Global Challenges.* **2019**, *3*:1800023–40.
72. Honghong, S.; Jing, Z.; Pengfei, S.; Yubing, X. Maize-like ionic liquid@polyaniline nanocomposites for high performance supercapacitor. *e-Polymers.* **2019**, *19*:313–22.
73. Pahovnik, D.; Zagar, E.; Vohlidal, J.; Zigon, M. Effect of cations on polyaniline morphology. *Chem Pap.* **2013**;67:946–51.

74. Al-Zohbi, F.; Ghamouss, F.; Schmaltz, B.; Abarbri, M.; Zaghrioui, M.; Tran-Van, F. Enhanced Storage Performance of PANI and PANI/Graphene Composites Synthesized in Protic Ionic Liquids. *Materials*. **2021**, *14*:4275–91.
75. Zhang, D.; Chen, Y.; Bai, X.; Li, X.; Ma, Y.; Chen, Z. Preparation and Electrochemical Testing of Polyaniline (PANI) Nanoparticles with Uniform Morphology and Good Dispersion in a Water-task-specific Ionic Liquid Medium. *Mater Sci*. **2019**, *25*:297–302.
76. Zhong, C.; Deng, Y.; Hu, W.; Qiao, J.; Zhang, L.; Zhang, J. A review of electrolyte materials and compositions for electrochemical supercapacitors. *Chem Soc Rev*. **2015**, *44*:7484–539.
77. Cheng, X.; Pan, J.; Zhao, Y.; Liao, M.; Peng, H. Gel Polymer Electrolytes for Electrochemical Energy Storage. *Adv Energy Mater*. **2017**, *8*:1702184.
78. Holbrey, J.D.; Seddon, K.R. Ionic Liquids. *Clean Products and Processes*. **1999**, *1*:223–36.
79. Rogers, R.D.; Seddon, K.R. Chemistry. Ionic liquids--solvents of the future? *Science*. **2003**, *302*:792–803.
80. Earle, M.J.; Seddon, K.R. Ionic Liquids: Green Solvents for the Future. *Clean Solvents: Am. Chem. Soc.* **2002**:10–25.
81. Lin, Z.; Taberna, P.-L.; Simon, P. Graphene-Based Supercapacitors Using Eutectic Ionic Liquid Mixture Electrolyte. *Electrochim Acta*. **2015**, *206*:446–51.
82. Mousavi, P.S.; Wilson, B.E.; Kashefolgheta, S.; Anderson, E.L.; He, S.; Buhlmann, P. et al. Ionic Liquids as Electrolytes for Electrochemical Double-Layer Capacitors: Structures that Optimize Specific Energy. *ACS Appl Mater Interfaces*. **2016**, *8*:3396–406.
83. Kim, C.H.; Wee, J.-H.; Kim, Y.A.; Yang, K.S.; Yang, C.-M. Tailoring the pore structure of carbon nanofibers for achieving ultrahigh-energy-density supercapacitors using ionic liquids as electrolytes. *J Mater Chem A*. **2016**, *4*:4763–70.
84. Huang, P.-L.; Luo, X.-F.; Peng, Y.-Y.; Pu, N.-W.; Ger, M.-D.; Yang, C.-H. et al. Ionic Liquid Electrolytes with Various Constituent Ions for Graphene-based Supercapacitors. *Electrochim Acta*. **2015**, *161*:371–7.
85. Forse, A.C.; Griffin, J.M.; Merlet, C.; Bayley, P.M.; Wang, H.; Simon, P. et al. NMR Study of Ion Dynamics and Charge Storage in Ionic Liquid Supercapacitors. *J Am Chem Soc*. **2015**, *137*:7231–42.
86. Aoki, A.; Umehara, R.; Banba, K. Conductive polyaniline/surfactant ion complex Langmuir-Blodgett films. *Langmuir*. **2009**, *25*:1169–74.
87. Lebedeva, M.V.; Gribov, E.N. Electrochemical behavior and structure evolution of polyaniline/carbon composites in ionic liquid electrolyte. *J Solid State Electrochem*. **2020**, *24*:739–51.
88. Ueki, T.; Watanabe, M. Macromolecules in Ionic Liquids: Progress, Challenges, and Opportunities. *Macromolecules*. **2008**, *41*:3739–49.
89. Kreuer, K.D.; Fuchs, A.; Ise, M.; Spaeth, M.; Maier, J. Imidazole and pyrazole-based proton conducting polymers and liquids. *Electrochim Acta*. **1998**, *43*:1281–8.
90. Cao, Z.; Xia, Y. Synthesis and tribological properties of polyaniline functionalized by ionic liquids. *J Mater Sci*. **2018**, *53*:7060–71.
91. Song, P.; Wang, H. High-Performance Polymeric Materials through Hydrogen-Bond Cross-Linking. *Adv Mater*. **2019**, *32*:1901244.
92. Qu, K.; Zeng, X. Ionic liquid-doped polyaniline and its redox activities in the zwitterionic biological buffer MOPS. *Electrochim Acta*. **2016**, *202*:73–83.

**Publisher's Note:** IIKII stays neutral with regard to jurisdictional claims in published maps and institutional affiliations.

**Copyright:** © 2021 The Author(s). Published with license by IIKII, Singapore. This is an Open Access article distributed under the terms of the [Creative Commons Attribution License](https://creativecommons.org/licenses/by/4.0/) (CC BY), which permits unrestricted use, distribution, and reproduction in any medium, provided the original author and source are credited.